Nanoscale Advances

ROYAL SOCIETY OF CHEMISTRY

PAPER

View Article Online
View Journal | View Issue

Cite this: *Nanoscale Adv.*, 2020, **2**, 1352

Porous nickel doped titanium dioxide nanoparticles with improved visible light photocatalytic activity

Bingbing Guan,†[a] Jie Yu,†[a] Siyao Guo,[b] Shen Yu[a] and Song Han *[a]

Received 6th December 2019
Accepted 23rd February 2020

DOI: 10.1039/c9na00760a

rsc.li/nanoscale-advances

A green hydrothermal synthesis route to prepare a porous nickel doped titanium dioxide (Ni–TiO_2) nanostructured photocatalyst has been developed in this research. The results show that Ni doping can greatly increase the visible light photocatalytic performance of TiO_2 through the introduction of impurity bands in the band gap of TiO_2. After 5 cycles of reuse, Ni–TiO_2 nanoparticles still show stable photocatalytic activity for MB degradation. The Ni–TiO_2 nanoparticles developed in the present study are expected to have great potential applications in wastewater treatment due to the advantages of strong visible light photocatalytic performance, a simple synthetic process and high cycle utilization performance.

1. Introduction

Due to the prosperity of modern industries, especially the ones dealing with plastics, paper and textile dying, a huge amount of wastewater with various kinds of effluents is discharged, resulting in a great crisis in the acquirement of fresh water.[1] Organic dye pollutants, one of the main produced effluents, can seriously disturb and destroy the ecological balance, leaving a heavy negative impact on the living, both human beings and plants.[2] To mitigate the above mentioned crisis, a great number of studies have focused on dye wastewater treatment, and various strategies have been developed, such as biodegradation,[3] chlorination,[4] electrochemical,[5] photocatalytic[6–10] and adsorption[11,12] methods. As one of the most effective methods, heterogeneous photocatalysis can greatly facilitate the oxidation of the pollutants and the by-products of hazardous organic pollutants.[12] These catalysts typically have an excellent capability to convert photon energy into chemical energy which is favorable for the decomposition of the main toxic organic contaminants. Among these catalysts, TiO_2 has been proved to be the most effective one due to its first usage in heterogeneous photocatalysis under UV light irradiation by Fujishima and Honda in 1972.[13] Afterwards, photocatalysis with TiO_2 catalysts became a research hotspot to decay the harmful chemical effluents present in wastewater.[14,15] After several decades of development, anatase TiO_2 is now considered to be one of the most common photocatalysts with high photocatalytic activity.[16]

TiO_2 has a favorable band gap, good chemical stability, good photostability, and high corrosion resistance.[17,18] TiO_2 is also one of the most noticeable photocatalysts with particular properties: it is a recoverable and reusable catalyst and can offer an eco-friendly and non-toxic approach for dye wastewater treatment. The photocatalytic activity of TiO_2 is based on the mechanism of the formation of electron/hole (e^-/h^+) pairs under the illumination of light which can initiate chemical reactions by generating radical species on the surface of TiO_2.[19] However, its poor efficiency in response to visible light limits its application due to the hindrance of the large band gap to catalyst efficiency under natural sunlight illumination which mostly contains visible regions.[20]

Doping of TiO_2 with different transition metals (Fe, Mn, Cu, Ni, *etc.*) can enhance the degradation under visible light irradiation, which has been successfully applied in wastewater treatment.[21] The reducing of the band gap of the catalysts has been achieved by doping metals through different processes. Benjwal *et al.* reported that a Zn and Mn co-doped TiO_2 photocatalyst showed high activity and excellent adsorption properties in low concentration aqueous solutions.[22] Copper phthalocyanine (CuPc) doped TiO_2 was confirmed to be an efficient and stable photocatalyst for degradation of methylene blue from aqueous solution under solar light irradiation.[23] The doping of TiO_2 with other transition metals such as Fe, Ni and Co has also been employed in various applications.[24–26] However, the applications of doped TiO_2 are still limited by their high cost and relatively low stability.

To obtain highly effective TiO_2 photocatalysts, the synthesis techniques need to be well controlled. In this work, novel Ni–TiO_2 nanoparticles have been developed using a green hydrothermal-synthesis route. Different from traditional TiO_2 preparation techniques, this synthesis route is easy to be operated and could save time. Meanwhile, the novel Ni–TiO_2 nanoparticles exhibit outstanding performance on adsorption

[a]*College of Forestry, Northeast Forestry University, Harbin 150040, China. E-mail: songh77@126.com*

[b]*School of Civil Engineering, Qingdao University of Technology, Qingdao 266033, China*

† These authors contributed equally.

of MB dye from aqueous solutions in darkness and high photocatalytic activity towards MB dye under visible light. The catalyst also exhibits extremely high cycle performance and recyclability. The synthesis strategy presented in this work can prepare materials with outstanding properties and will show potential application in water treatment systems.

2. Experimental

2.1 Materials

Butyl titanate ($[CH_3(CH_2)_3O]_4Ti$), absolute ethyl alcohol (C_2H_5OH), hydrochloric acid (HCl), ammonium hydroxide ($NH_3 \cdot H_2O$), nickel nitrate ($Ni(NO_3)_2 \cdot 6H_2O$), and methylene blue (MB), were all purchased from Sinopharm Reagent Co Ltd. All the chemicals were of analytical grade and used without further purification. Deionized water was used throughout for the preparation of all the experimental solutions.

2.2 Preparation of TiO_2 and Ni–TiO_2 nanoparticles

Tetrabutyl titanate (10 mL) and absolute ethyl alcohol (10 mL) were mixed to obtain solution A. Absolute ethyl alcohol (20 mL) and deionized water (100 mL) were mixed to obtain solution B. Solution A was then added into solution B dropwise under magnetic stirring for 30 min. Then, the pH value was adjusted to 9 by ammonium hydroxide. After homogenization for 30 min, the mixed solution was transferred into a Teflon-lined autoclave for crystallization at 140 °C for 4 h. The resulting product was washed with ethyl alcohol and deionized water 3 times each. Then the nanoparticles were separated from the liquid phase by centrifugation to remove the remaining compounds. The final product was dried at 80 °C overnight to obtain TiO_2 powders. The synthetic steps for Ni-(3 wt%) TiO_2 nanoparticles were little different from the above. In step three, solution A and a nickel nitrate solution (0.85 mL, 1 mol L^{-1}) were added into solution B dropwise under magnetic stirring for 30 min.

2.3 Characterization

FT-IR spectra were recorded using a Shimadzu instrument (model 8400S) in the region 4000–400 cm^{-1}. The phase analysis of the as-synthesized products was carried out using X-ray diffraction (XRD, DX-2700) with Cu-Kα radiation (λ = 1.5406 Å). UV-vis-NIR absorption spectra of the samples were recorded using a UV-1800 spectrophotometer (Shimadzu). SEM images were obtained using a S-4800 instrument (Hitachi, Japan). The specific surface area was calculated by the Brunauer–Emmett–Teller (BET) method, and the pore size distribution was obtained using the Barrett–Joyner–Halenda (BJH) model using a Micromeritics ASAP 2020 adsorption analyzer.

2.4 Photocatalytic experiments

Degradation of MB was used as an indicator for the photocatalytic activity of the TiO_2 nanoparticles. The prepared TiO_2 nanoparticles were immersed in 10 mg L^{-1} MB solution and were allowed to completely equilibrate with MB for 20 min in darkness. Then the system was irradiated by simulated solar light (Xe lamp, 300 W) or UV light. 10 mL of solution was taken and analysed at different reaction times (every 15 min) using a UV-1800 spectrophotometer.

3. Results and discussion

3.1 FTIR spectra

Fig. 1 shows the FTIR spectra of the TiO_2 and Ni–TiO_2 nanoparticles. The strong absorption bands at 662 and 704 cm^{-1} might be due to the Ti–O vibrations in the TiO_2 lattice. Furthermore, a broad absorption band in the region of 3000–3500 cm^{-1} can be assigned to the surface-bound hydroxyl groups and their stretching vibration on the surface of TiO_2.[27] A second adsorption band at 1000–1700 cm^{-1} is assigned to surface-adsorbed water molecules (H–O–H bending, 1633 cm^{-1}).[28] It can confirm a strong interaction of water molecules with the TiO_2 surface to form a number of broad OH– stretching vibrations.[22] A broad intense vibration region at 1000–1200 cm^{-1} is credited to the Ti–O–Ti vibration. Moreover, occurrence of bands between 1300–1500 cm^{-1} for Ni–TiO_2 nanoparticles indicates the presence of a small amount of organic material in the sample.[29] With an increase in Ni concentration, the shift to lower wavenumbers of the Ti–O–Ti band could be attributed to the increase in powder particle size.[30]

3.2 Phase analysis and morphology

XRD patterns of TiO_2 and Ni–TiO_2 nanoparticles are shown in Fig. 2A. The Ni–TiO_2 sample exhibits peaks at 25.28°, 37.80°, 48.05°, 53.89°, 55.06°, 62.69°, 70.31°, and 75.03°, corresponding to the anatase phase (JCPDF 21-1272), with no other phases. In addition, peaks corresponding to Ni oxides are not detected. These results further indicate that Ni ions have been successfully doped into TiO_2 nanoparticles.[2] Fig. 2B shows the spherically shaped Ni doped TiO_2 nanostructures. Compared with the pure TiO_2 image (Fig. 2C), Ni–TiO_2 shows homogeneous nanoparticles with sizes of 20–30 nm.

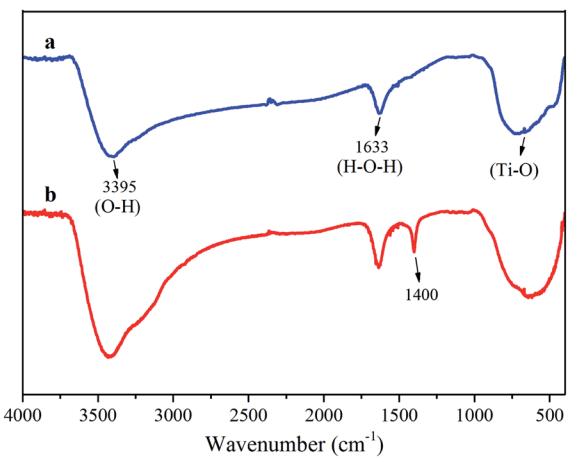

Fig. 1 FT-IR spectral analysis of (a) TiO_2 and (b) Ni–TiO_2 nanoparticles.

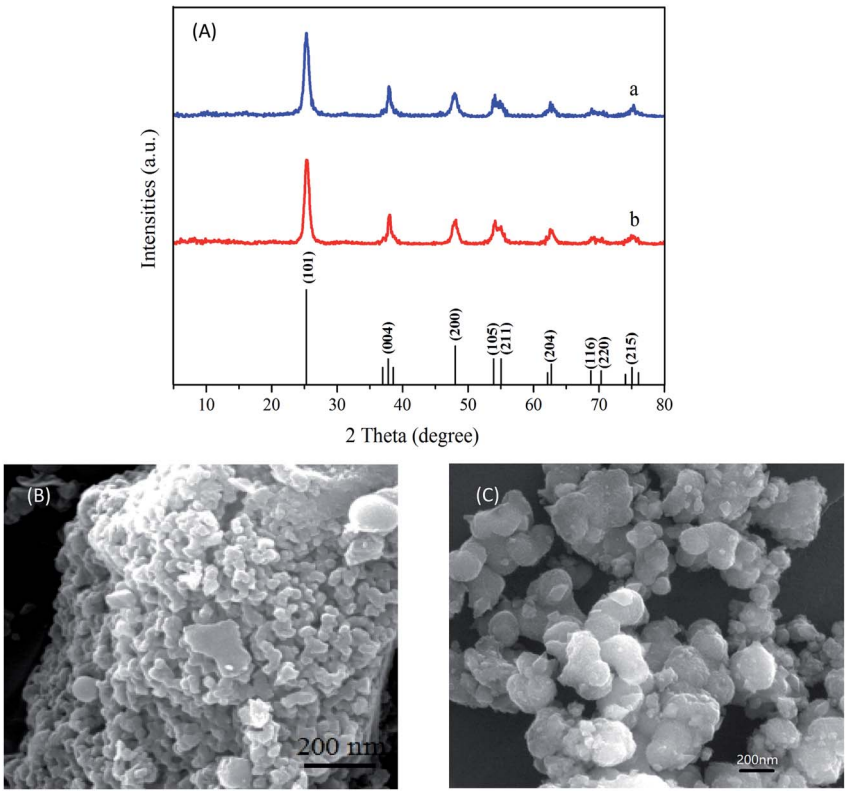

Fig. 2 (A) XRD patterns of (a) TiO_2 and (b) Ni–TiO_2 nanoparticles; (B) morphology of Ni–TiO_2; (C) morphology of TiO_2.

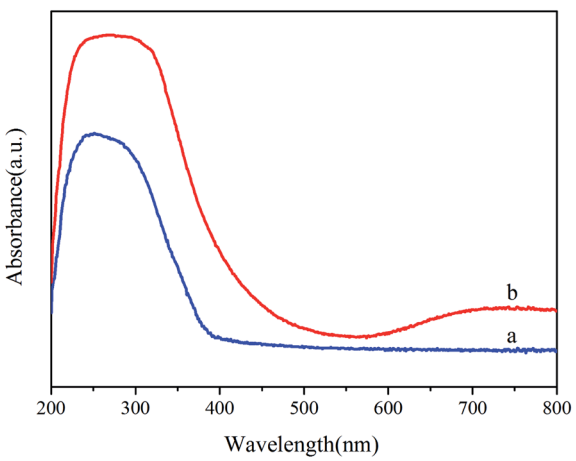

Fig. 3 UV-visible absorption spectra of (a) TiO_2 and (b) Ni–TiO_2 samples.

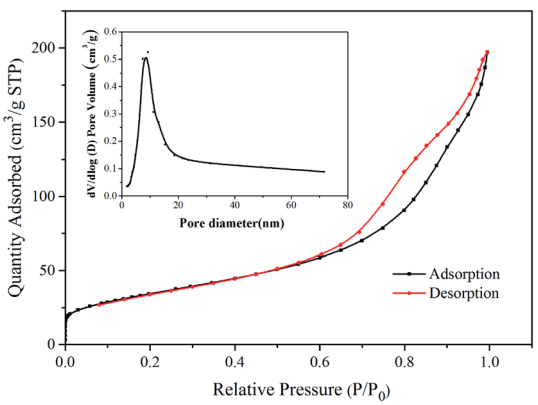

Fig. 4 Nitrogen adsorption–desorption isotherms and pore size distribution curve of Ni–TiO_2.

3.3 UV-vis spectral analysis

The electronic structure of the samples that furnishes the optical properties (*e.g.*, absorption and band gap) through the irradiating light intensity was determined by UV-vis spectral analysis,[17] as shown in Fig. 3. In the absorption spectra, it is noticeable that the optical absorption edge of the pure TiO_2 is at 400 nm. The band gap of TiO_2 is 3.21 eV which is favorable to produce electron–hole pairs under the UV light irradiation. However, the pure TiO_2 can not degrade dyes under visible light. Compared to pure TiO_2, Ni–TiO_2 nanoparticles exhibit a broad absorption covering the range as shown in Fig. 3b, which can be ascribed to the doping energy levels caused by the doped Ni in the band gap of TiO_2.

3.4 Nitrogen adsorption–desorption isotherm of Ni–TiO_2

The nitrogen adsorption–desorption isotherm and BJH pore size distribution curve (inset) of Ni–TiO_2 are shown in Fig. 4, which displays a type-IV isotherm with a specific surface area of 124.02 $m^2\ g^{-1}$. This implies that the pores within the materials are mainly within the mesoporous range. The pore size distribution

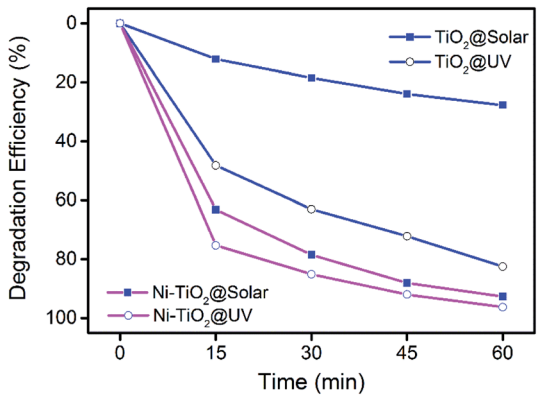

Fig. 5 Photodegradation of MB dye using TiO_2 and Ni–TiO_2 nanoparticles under UV and solar light irradiation.

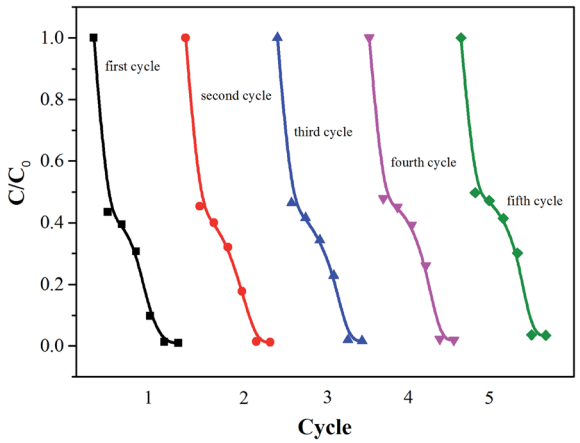

Fig. 6 Photocatalytic stability test of Ni–TiO_2 nanoparticles.

is calculated using the BJH method (desorption curve).[31] The pore-size distribution of Ni–TiO_2 shows that the pore diameters distribution (Fig. 4 inset) has a peak at about 9 nm, indicating that Ni–TiO_2 has a mesoporous structure. These small pores can enhance photocatalytic activities by favoring the adsorption of small dye molecules on the active surface.

3.5 MB decomposition capacity under solar and UV light

Fig. 5 depicts the photocatalytic degradation of MB using TiO_2 and Ni–TiO_2 nanoparticles under UV and solar light irradiation as a function of time with an initial MB concentration of 10 mg L^{-1}. The degradation efficiencies of Ni–TiO_2 nanoparticles under solar and UV after 60 min irradiation are found to be 92.7% and 96.3%, respectively. However, the corresponding degradation efficiencies are only 85.9% and 27.7% for pure TiO_2. It can be found that Ni doping can increase the visible light degradation performance greatly. The TiO_2 catalyst shows very weak photocatalytic performance for MB degradation under solar light irradiation. After Ni doping, the visible light photocatalytic performance increases to a similar level compared with that under UV light. The result demonstrates that Ni doping can improve the photocatalytic activity of TiO_2 nanoparticles under visible light.

3.6 Photocatalytic performance stability

The stability is also important for the practical application of the photocatalyst. Therefore, the cyclic stability of Ni–TiO_2 nanoparticles was investigated by monitoring the catalytic activity during successive cycles of degradation. As shown in Fig. 6, after a five cycles test, the Ni–TiO_2 nanoparticles exhibit a very stable photocatalytic performance without any significant deactivation, thereby demonstrating high stability after multiple reuse cycles.

3.7 Photocatalytic mechanism of Ni–TiO_2

The plausible mechanism of the photocatalytic activity of the synthesized Ni–TiO_2 nanoparticles can be explained by the energy band gap structure of TiO_2 shown in Fig. 7. The direct excitation of an electron from the valence band (VB) to the conduction band (CB) in the presence of visible light is not possible due to the broad band gap (3.21 eV) of pure TiO_2. Through the incorporation of Ni ions into the TiO_2 lattice, the band gap of TiO_2 decreases due to the formation of impurity levels below the CB in the band gap, then the electrons can transfer from the VB to these energy levels. These electrons travel to the surface and are adsorbed by O_2 and produce $^{\bullet}O_2$

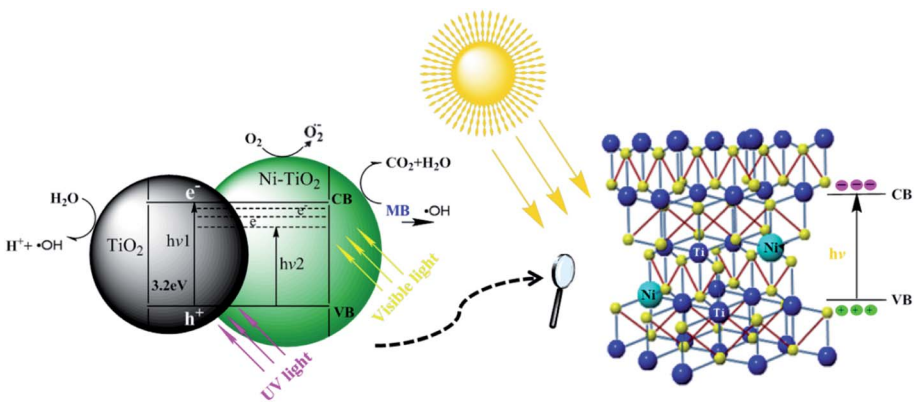

Fig. 7 Possible mechanism of the MB degradation by Ni–TiO_2 nanoparticles.

ions, which can further convert to the strong redox species $^{\bullet}OH$ ions.[32] These redox ions are responsible for the degradation of the surface adsorbed hazardous MB.[22]

4. Conclusions

Ni–TiO_2 nanoparticles were synthesized by a green hydrothermal-synthesis route and characterized in detail. The activities of the synthesized nanoparticles were studied through MB photocatalytic degradation. The results demonstrate that Ni doping can greatly increase the visible light photocatalytic performance of TiO_2 through the introduction of impurity bands in the band gap of TiO_2. After 5 cycles of reuse, Ni–TiO_2 nanoparticles still show stable photocatalytic activity for MB degradation. Thus the Ni–TiO_2 nanoparticles developed in the present study are expected to have great potential applications in wastewater treatment due to the advantages of strong visible light photocatalytic performance, a simple synthetic process and high cycle utilization performance.

Conflicts of interest

There are no conflicts to declare.

Acknowledgements

The authors gratefully acknowledge the support from National Natural Science Foundation of China (51478406, 51508293), 973 Program (2015CB6555100), 111 Program and Qingdao Applied Research Project (17-1-1-87-jch).

References

1 T. M. David, P. Wilson, R. Mahesh, S. Dhanavel, S. Hussain, S. J. M. Boby, A. Stephen, C. Ramesh and P. Sagayaraj, Investigating the photocatalytic degradation property of Pt, Pd and Ni nanoparticles-loaded TiO_2 nanotubes powder prepared via rapid breakdown anodization, *Environ. Technol.*, 2017, **1**, 1479–1487.

2 X. H. Li, Y. Wu, Y. H. Shen, Y. Sun, Y. Yang and A. J. Xie, A novel bifunctional Ni-doped TiO_2 inverse opal with enhanced SERS performance and excellent photocatalytic activity, *Appl. Surf. Sci.*, 2018, **427**, 739–744.

3 C. Yang, J. S. Yu, Q. S. Li and Y. M. Yu, Facile synthesis of monodisperse porous ZnO nanospheres for organic pollutant degradation under simulated sunlight irradiation: the effect of operational parameters, *Mater. Res. Bull.*, 2017, **87**, 72–83.

4 S. Yaparatne, C. P. Tripp and A. Amirbahman, Photodegradation of taste and odor compounds in water in the presence of immobilized TiO_2–SiO_2 photocatalysts, *J. Hazard. Mater.*, 2018, **346**, 208–217.

5 S. Kumar, B. Ahmed, A. K. Ojha, J. Das and A. Kumar, Facile synthesis of CdO nanorods and exploiting its properties towards supercapacitor electrode materials and low power UV irradiation driven photocatalysis against methylene blue dye, *Mater. Res. Bull.*, 2017, **90**, 224–231.

6 S. Y. Guo, S. Han, B. Chi, J. Pu and J. Li, Structurally controlled ZnO/TiO_2 heterostructures as efficient photocatalysts for hydrogen generation from water without noble metals: The role of microporous amorphous/crystalline composite structure, *J. Power Sources*, 2014, **245**, 979–985.

7 S. Y. Guo, T. J. Zhao, J. Z. Quan and S. Han, Self-assembly synthesis of precious-metal-free 3D ZnO nano/micro spheres with excellent photocatalytic hydrogen production from solar water splitting, *J. Power Sources*, 2015, **293**, 17–22.

8 S. Y. Guo, S. Han, B. Chi, J. Pu and J. Li, A facile low-temperature approach to designing controlled amorphous-based titania composite photocatalysts with excellent noble-metal-free photocatalytic hydrogen production, *ACS Appl. Mater. Interfaces*, 2014, **6**, 4743–4751.

9 S. Y. Guo, S. Han, B. Chi, J. Pu and J. Li, Synthesis and characterization of nitrogen and phosphate codoped titanium dioxide with excellent visible-light photocatalytic activity, *J. Alloys Compd.*, 2012, **544**, 50–54.

10 A. A. Ismail, I. Abdelfattah, M. Faisal and A. Helal, Efficient photodecomposition of herbicide imazapyr over mesoporous Ga_2O_3–TiO_2 nanocomposites, *J. Hazard. Mater.*, 2018, **342**, 519–526.

11 L. N. Liu, J. G. Dai, T. J. Zhao, S. Y. Guo, D. S. Hou, P. Zhang, J. Shang, S. Wang and S. Han, A novel Zn(II) dithiocarbamate/ZnS nanocomposite for highly efficient Cr^{6+} removal from aqueous solutions, *RSC Adv.*, 2017, **7**, 35075–35085.

12 D. Zhao, G. Sheng, C. Chen and X. Wang, Enhanced photocatalytic degradation of methylene blue under visible irradiation on graphene@TiO_2 dyade structure, *Appl. Catal., B*, 2012, **111–112**, 303–308.

13 A. Fujishima and K. Honda, Photolysis-decomposition of water at surface of an irradiated semiconductor, *Nature*, 1972, **238**, 37–38.

14 J. Schneider, M. Matsuoka, M. Takeuchi, J. Zhang, Y. Horiuchi, M. Anpo and D. W. Bahnemann, Understanding TiO_2 photocatalysis: mechanisms and materials, *Chem. Rev.*, 2014, **114**, 9919–9986.

15 M. Ahmed and X. Guo, A review of metal oxynitrides for photocatalysis, *Inorg. Chem. Front.*, 2016, **3**, 578–590.

16 R. W. Matthews, Photocatalytic oxidation of organic contaminants in water: an aid to environmental preservation, *Pure Appl. Chem.*, 1992, **64**, 1285–1290.

17 A. A. Ismail, I. Abdelfattah, A. Helal, S. A. Al-Sayari, L. Robben and D. W. Bahnemann, Ease synthesis of mesoporous WO_3–TiO_2 nanocomposites with enhanced photocatalytic performance for photodegradation of herbicide imazapyr under visible light and UV illumination, *J. Hazard. Mater.*, 2016, **307**, 43–54.

18 X. Yang, L. Zhao, K. Lv, B. Dong and S. Wang, Enhanced efficiency for dye-sensitized solar cells with ZrO_2 as a barrier layer on TiO_2 nanofibers, *Appl. Surf. Sci.*, 2019, **469**, 821–828.

19 W. He, Z. Fang, K. Zhang, X. Li, D. Ji, X. Jiang, C. Qiu and K. Guo, Continuous synthesis of a co-doped TiO_2 photocatalyst and its enhanced visible light catalytic

activity using a photocatalysis microreactor, *RSC Adv.*, 2015, **5**, 54853–54860.

20 W. H. Feng, J. Z. Fang, L. X. Zhang, S. Y. Lu, S. X. Wu, C. Cheng, Y. Chen, Y. Ling and Z. Q. Fang, Plasmonic metallic Bi deposited $Bi_{12}SiO_{20}$ crystals with rich oxygen vacancies for enhanced photocatalytic degradation of RhB and 2,4-DCP, *Mater. Res. Bull.*, 2017, **94**, 45–53.

21 S. N. R. Inturi, T. Boningari, M. Suidan and P. G. Smirniotis, Visible-light-induced photodegradation of gas phase acetonitrile using aerosol-made transition metal (V, Cr, Fe, Co, Mn, Mo, Ni, Cu, Y, Ce, and Zr) doped TiO_2, *Appl. Catal., B*, 2014, **144**, 333–342.

22 P. Benjwal and K. K. Kar, Removal of methylene blue from wastewater under a low power irradiation source by Zn, Mn co-doped TiO_2 photocatalysts, *RSC Adv.*, 2015, **5**, 98166–98176.

23 B. Cabir, M. Yurderi, N. Caner, M. S. Agirtas, M. Zahmakiran and M. Kaya, Methylene blue photocatalytic degradation under visible light irradiation on copper phthalocyanine-sensitized TiO_2 nanopowders, *Mater. Sci. Eng., B*, 2017, **224**, 9–17.

24 G. Murtaza, R. Ahmad, M. S. Rashid, M. Hassan, A. Hussnain, M. AzharKhan, M. E. Ul Haq, M. A. Shafiqu and S. Riaz, Structural and magnetic studies on Zr doped ZnO diluted magnetic semiconductor, *Curr. Appl. Phys.*, 2014, **14**, 176–181.

25 W. Zhang, W. Zhou, J. H. Wright, Y. N. Kim, D. Liu and X. Xiao, Mn-doped TiO_2 nanosheet-based spheres as anode materials for lithium-ion batteries with high performance at elevated temperatures, *ACS Appl. Mater. Interfaces*, 2014, **6**, 7292–7300.

26 D. Das, D. Banerjee, B. Das, N. S. Das and K. K. Chattopadhyay, Effect of cobalt doping into graphitic carbon nitride on photo induced removal of dye from water, *Mater. Res. Bull.*, 2017, **89**, 170–179.

27 R. Sharma and K. K. Kar, Effects of structural disorder and nitrogen content on the oxygen reduction activity of polyvinylpyrrolidone-derived multi-doped carbon, *J. Mater. Chem. A*, 2015, **3**, 11948–11959.

28 W. C. Hung, S. H. Fu, J. J. Tseng, H. Chu and T. H. Ko, Study on photocatalytic degradation of gaseous dichloromethane using pure and iron ion-doped TiO_2 prepared by the sol-gel method, *Chemosphere*, 2007, **66**, 2142–2151.

29 P. Singla, O. P. Pandey and K. Singh, Study of photocatalytic degradation of environmentally harmful phthalate esters using Ni-doped TiO_2 nanoparticles, *Int. J. Environ. Sci. Technol.*, 2016, **13**, 849–856.

30 H. Khojasteh, M. S. Niasari and S. M. Derazkola, Synthesis, characterization and photocatalytic properties of nickel-doped TiO_2 and nickel titanate nanoparticles, *J. Mater. Sci.: Mater. Electron.*, 2016, **27**, 3599–3607.

31 A. Ajmal, I. Majeed, R. N. Malik, H. Idriss and M. A. Nadeem, Principles and mechanisms of photocatalytic dye degradation on TiO_2 based photocatalysts: a comparative overview, *RSC Adv.*, 2014, **4**, 37003–37026.

32 E. O. Oseghe, P. G. Ndungu and S. B. Jonnalagadda, Synthesis ofmesoporous Mn/TiO_2 nanocomposites and investigating the photocatalytic properties in aqueous systems, *Environ. Sci. Pollut. Res.*, 2015, **22**, 211–222.